PAPER

Check for updates

Non-close-packed arrangement of soft elastomer microspheres on solid substrates†

Yuma Sasaki, [ID] [a] Seina Hiroshige, [ID] [a] Masaya Takizawa, [ID] [a] Yuichiro Nishizawa, [ID] [a] Takayuki Uchihashi, [ID] [bc] Haruka Minato [ID] [a] and Daisuke Suzuki [ID] *[ad]

Unlike rigid microparticles, soft and deformable elastomer (rubber) microspheres were found to exhibit a non-close-packed arrangement on solid substrates after the evaporation of water from their dispersions. The microscopic observation revealed that individual microspheres are ordered in regular intervals at the air/water interface of a sessile droplet and remain fixed on the substrate without being affected by the capillary forces during evaporation due to their deformability. Moreover, using the Langmuir–Blodgett method, thin films of non-close-packed structures could be successfully generated over large areas. Our findings may potentially help to control the arranged structures of elastomer microspheres, which can be expected to improve the nano-science and technology for the precise control for *e.g.* surface patterning.

Introduction

The arrangements of uniformly sized nano- and microspheres on solid substrates, including organic (*e.g.*, polystyrene, PS) and inorganic (*e.g.*, silica or gold) spheres,[1–6] give rise to important properties of functional materials, such as optical properties,[7–9] water repellency,[10,11] and biocompatibility.[12,13] Therefore, such colloidal arrays play a crucial role in many applications, including inkjet printing,[14,15] biosensors,[16] films,[17–22] lithography,[23–25] and biomaterials.[26,27] To further develop these functions, precise control of these arrangements is required.

One of the simplest and most cost-effective methods to produce such colloidal arrays is the controlled evaporation of sessile droplets that contain colloidal particles on solid substrates.[28–34] In general, colloidal particles, such as polystyrene (PS) and silica, are partially arranged on solid substrates after evaporation of their dispersions.[35–37] These partially ordered structures are closely packed and neighboring particles are in contact with each other.

Against this background, we unexpectedly found that soft and deformable elastomer (rubber) microspheres can form

‘non-close-packed’ ordered structures on solid substrates upon evaporating water from sessile aqueous droplets without applying any treatment such as exposure to plasma[38–40] or heat.[41]

Results and discussion

First, microspheres of the elastomers, poly(butyl acrylate) (pBA; $T_g = -53$ °C) or poly(ethyl acrylate) (pEA; $T_g = -23$ °C), were synthesized *via* surfactant-free emulsion polymerization in the absence (or presence) of the crosslinker divinylbenzene (DVB).

The microspheres are denoted as BA(X)Y or EA(X)Y, where X and Y indicate the DVB concentration (mol%) in the microspheres and the hydrodynamic diameter calculated from dynamic light scattering (DLS, nm), respectively. All elastomer microspheres were purified by dialysis and centrifugation before use, and the properties of all microspheres used in this study are listed in Table S1.†

We initially evaluated the macroscopic structures obtained upon evaporation of water from an aqueous dispersion of BA(0) 710 (0.06 wt%, 30 μL) at room temperature (~25 °C, ~30% humidity) on a glass substrate. The resulting thin film was mostly uniform and transparent (Fig. 1a). Regardless of the particle concentration, a ring-like stain was observed in the dried thin films due to the coffee-ring effect (Fig. 1a and S1†).[35] In addition, a white region appeared near the center of the films with increasing particle concentration; the microspheres were more concentrated in this area of the film because water was present in this region up until the complete evaporation of the droplet. Subsequently, the microscopic structure of the film was observed using optical microscopy. Surprisingly, the BA(0)710 microspheres formed an ordered non-close-packed structure

[a]Graduate School of Textile Science & Technology, Shinshu University, 3-15-1 Tokida, Ueda, Nagano 386-8567, Japan. E-mail: d_suzuki@shinshu-u.ac.jp

[b]Department of Physics, Structural Biology Research Center, Graduate School of Science, Nagoya University, Furo-cho, Chikusa-ku, Nagoya, Aichi 464-8602, Japan

[c]Exploratory Research Center on Life and Living Systems, National Institutes of Natural Sciences, 5-1 Higashiyama, Myodaiji, Okazaki, Aichi 444-8787, Japan

[d]Research Initiative for Supra-Materials, Interdisciplinary Cluster for Cutting Edge Research, Shinshu University, 3-15-1 Tokida, Ueda, Nagano 386-8567, Japan

† Electronic supplementary information (ESI) available: Experimental details, photographs, optical microscopy images, and movies, as well as analysis of the adsorption behavior at the air/water interface, center-to-center distance of the adsorbed microspheres on the substrates, and pair correlation functions. See DOI: 10.1039/d1ra02688g
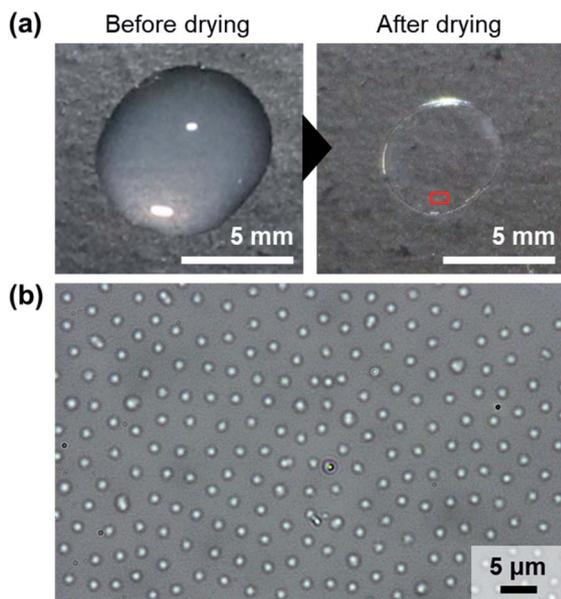
Paper   RSC Advances

Fig. 1 (a) Photographs of a sessile droplet and a dried thin film containing BA(0)710 microspheres. The droplets were dried on a glass substrate at room temperature (~25 °C, ~30% humidity). The microsphere concentration was 0.06 wt%. (b) Representative optical microscopy image of the dried BA(0)710 dispersion on a glass substrate.

partially on the substrate (Fig. 1b and S2†). It is worth noting that the formation of ordered structures of elastomer microspheres on solid substrates was observed independently of the size and chemical species of the elastomer microspheres (Fig. 2 and S3†), as well as independently of the charge and chemical composition of the substrates (Fig. S4†), but was dependent on their degree of crosslinking; for example, BA(5)340 did not show this type of structure (Fig. 2 and S3†). Moreover, the elastomer microspheres aggregated in the presence of increasing concentrations of sodium chloride (Fig. S5†).
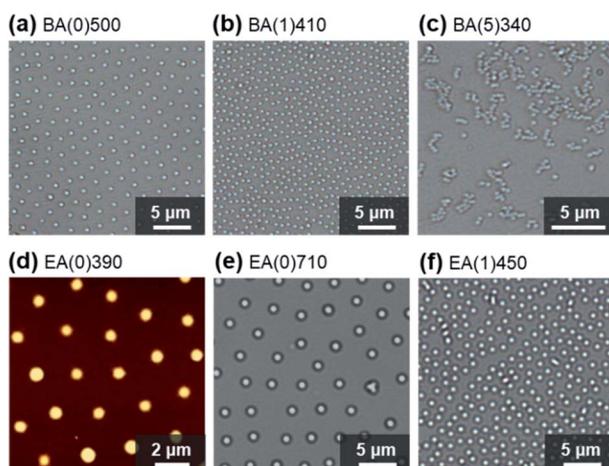

Fig. 2 (a–c, e and f) Optical microscopy and (d) atomic force microscopy images of thin films of the elastomer microspheres after drying dispersion droplets on glass substrates. The droplets were dried at room temperature (~25 °C, ~30% humidity).

To clarify the mechanism of the formation of the non-close-packed elastomer microsphere array, the drying behavior of the dispersions was microscopically investigated (Fig. 3a). Individual EA(0)710 microspheres were observed at the air/water interface at the center of the sessile droplet (10 μL) during evaporation (Fig. 3b). At the late stage of drying (normalized time (T_N) = ~0.85; $T_N = T/T_{dried}$, where T and T_{dried} denote an arbitrary time and the time required for complete drying, respectively[32,33]), the EA(0)710 microspheres were immediately adsorbed and ordered at intervals at the air/water interface without aggregation on account of dipole–dipole interactions that originate from repulsion between the dipole moment of
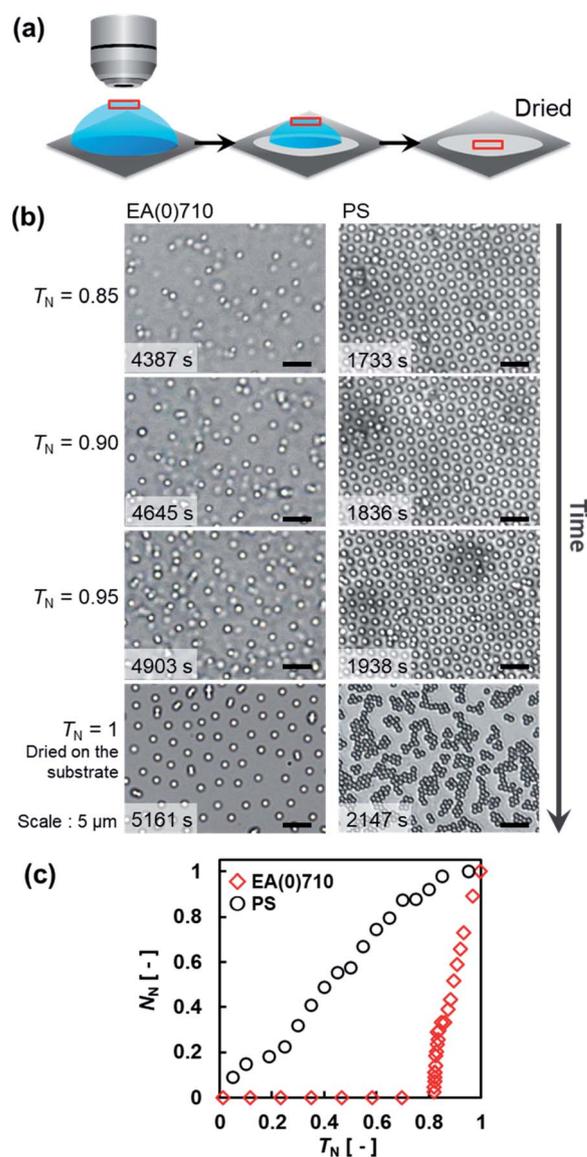

Fig. 3 (a) Schematic illustration of the observation of evaporation of the sessile droplets. (b) Optical microscopy images of EA(0)710 and PS microspheres at the air/water interface at the center of each droplet on the glass substrate during evaporation. The initial concentration of particles in the droplets was 0.05 wt% (EA(0)710; Movie S1, ESI†) or 0.08 wt% (PS; Movie S2†). (c) Normalized amount of adsorbed microspheres, N_N, as a function of T_N.
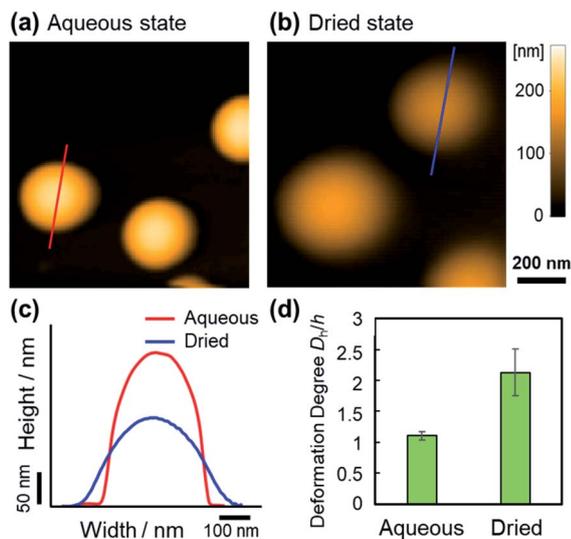
Fig. 4 AFM height images of the EA(0)260 microspheres ($D_h = 256$ nm) (a) in the aqueous state and (b) in the dried state on a positively charged mica substrate. (c) Cross-sections of representative microspheres in the aqueous or dried state. (d) Degree of deformation ($=D_h/h$) of the microspheres.

each microsphere (Fig. 3b).[42] The normalized amount of the microspheres adsorbed at the air/water interface, N_N ($N_N = N/N_{dried}$, where N and N_{dried} denote the amount of microspheres adsorbed at an arbitrary point in the drying process and the amount adsorbed at complete drying per unit of interfacial area[32,33]) increased until complete drying occurred (Fig. 3c). Additionally, the center-to-center distance of the EA(0)710 microspheres adsorbed at the interface gradually decreased due to the increasing number of adsorbed microspheres and the compression of the surface as the evaporation of water proceeded and the total surface area decreased (Fig. 3c, S6 and Movie S1†). Finally, the structure in which the microspheres were arranged at intervals on the interface were transferred onto the substrate during drying ($T_N \sim 1$) with almost no structural disruption (Fig. 3b, EA(0)710, Movie S1†).

It has been reported that PS microspheres adsorbed at the air/water interface where a meniscus is formed on the edge of a glass circular container are uniformly ordered at intervals due to dipole–dipole interactions between neighboring PS microspheres.[42] We also observed the ordering of PS microspheres at intervals due to dipole–dipole interactions at the air/water interface of a sessile droplet (Fig. 3b, PS, Fig. S7†). However, the arrangement of the PS microspheres at the interface was not transferred to the substrate without disruption during drying (Fig. 3b, PS, $T_N \sim 1$, Movie S2†), possibly due to capillary forces.

Our results indicate that the deformability of the microspheres is a key factor for the formation of thin films with an ordered particle structure. Therefore, we investigated the deformability of a single microsphere adsorbed on a solid substrate in water and in a dry environment using atomic force microscopy (AFM), which can evaluate the nanostructure of soft microspheres.[43–47] The heights (h) of the EA(0)260 elastomer microspheres were calculated from the cross-sections of the

AFM height images and found to be 232 nm in water and 120 nm in the dry environment on the substrate (Fig. 4a–c). The degree of deformation ($=D_h/h$, where D_h denotes the hydrodynamic diameter calculated by DLS) increased from 1.1 in the aqueous environment to 2.1 in the dry environment (Fig. 4d). Although AFM measurements do not allow the observation of the drying behavior of the microspheres adsorbed on the substrate during evaporation, the difference in the degree of deformation suggested that the elastomer microspheres were deformed at the moment that the water completely evaporated.

Given that softer microspheres can quickly adsorb and immediately deform at a solid surface,[48] the adsorption energy of the deformed elastomer microspheres on the substrate increases with increasing contact area, as proposed by the JKR theory.[49] Hence, unlike the rigid PS microspheres that hardly deform at room temperature, the adsorbed and deformed elastomer microspheres remained fixed on the substrate without being affected by the
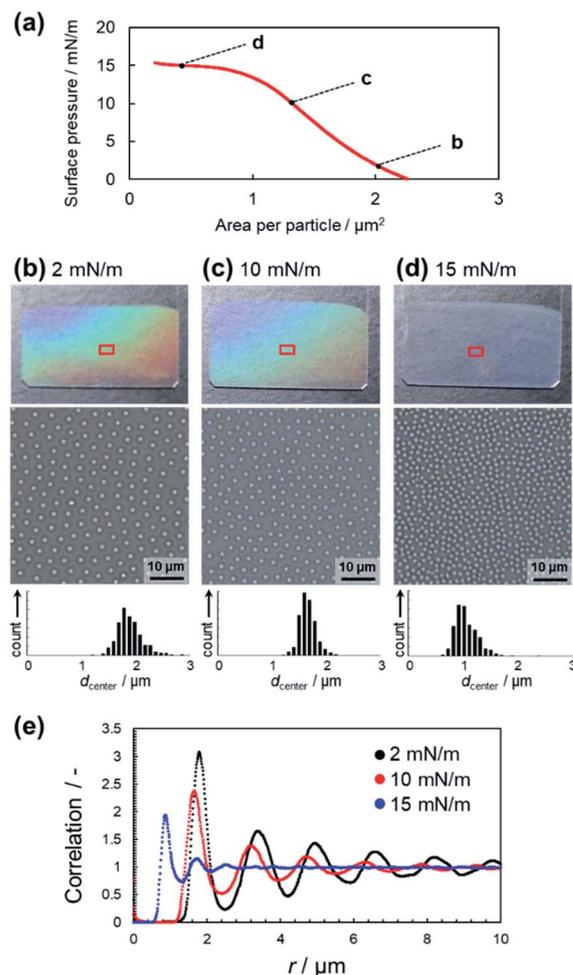

Fig. 5 (a) Compression isotherm of EA(1)450 microspheres at the air/water interface of a Langmuir trough. (b–d) Macroscopic and microscopic images and histograms of the center-to-center distance of the microspheres of the obtained films on glass substrates at 2 mN m⁻¹, 10 mN m⁻¹, and 15 mN m⁻¹, respectively. (e) Pair correlation function of the non-close-packed arrays of EA(1)450 microspheres on the glass substrate.

capillary forces during the evaporation of water, and their non-close-packed structures at the air/water interface were maintained on the substrate after drying due to an increased adsorption energy that can be rationalized using JKR theory.[49]

During the drying process of the sessile droplets, the adsorption behavior at the whole air/water interface is not homogeneous due to, *e.g.*, the coffee ring effect. Thus, to form the non-close-packed structures over large areas, the Langmuir–Blodgett method, which has the potential to modify the substrate with high reproducibility, was used with its horizontal air/water interface. Elastomer microspheres adsorbed at the air/water interface of a Langmuir trough were compressed by moving the barrier and thus transported on the substrate by lifting at the adjusted surface pressure (Fig. 5a). The monolayer films (~2.6 cm^2) obtained at surface pressures of 2 mN m^{-1} and 10 mN m^{-1} showed iridescence due to the uniform non-close-packed array structures formed by the elastomer microspheres (Fig. 5b and c). On the other hand, the highly compressed microspheres (*e.g.*, 15 mN m^{-1}) did not exhibit structural color due to their decreased orientation (Fig. 5d and e). When the soft non-crosslinked EA(0) 710 microspheres were used, structural color was not observed due to the high deformation, although the microspheres were uniformly ordered (Fig. S8†). As a result, we could successfully achieve the controlling a non-close-packed ordered microsphere structure by tuning the surface pressure. Our findings have the potential to enable control over the packing density and structure of elastomer microspheres without the use of complex techniques such as plasma or heat treatment. This method can thus be expected to improve techniques for the precise control of surface patterning, which is important for the advancement of nanoscience and nanotechnology.

Conclusions

In conclusion, ordered non-close-packed arrays of elastic pBA or pEA microspheres were obtained by simple drying of a sessile droplet of an aqueous dispersion of the microspheres. Observing the drying process of the dispersions revealed that the uniformly ordered structure of the elastomer microspheres at intervals on the air/water interface was successfully transferred onto the solid surface at the moment when the water completely evaporated, and that this behavior originates from the deformability of the microspheres. Moreover, non-close-packed microsphere arrangements were achieved over a larger area by tuning the surface pressure of the air/water interface where the microspheres were adsorbed using the Langmuir–Blodgett method. Therefore, these new findings regarding the formation of thin films composed of a non-close-packed arrangement of microspheres may lead to the creation of new applications that require thin layers of functional elastic materials.

Experimental

Materials

Ethyl acrylate (EA, 97%), *n*-butyl acrylate (BA, 98%), styrene (99%), 2,2-azobis(2-methylpropionamidine)dihydrochloride (V-50, 97%), potassium peroxodisulfate (KPS, 95%), ethanol (99.5%), and methanol (99.8%) were purchased from FUJIFILM Wako Pure Chemical Corporation (Japan) and used as received. Divinylbenzene (DVB, 80%) and (3-aminopropyl)-triethoxysilane (APTES, 97%) were purchased from Sigma Aldrich and used as received. Water in the present study was distilled and ion-exchanged (EYELA, SA-2100E1, Japan). All Glass substrates (24 mm × 60 mm/Neo Micro Cover Glass, Matsunami Glass Ind., Ltd.) were used after cleaning by ultra-sonication in (1) ethanol, (2) detergent in water, and (3) pure water.[32] PS substrate (60 mm/Non-Treated Dish, Iwaki, Asahi Glass Co., Ltd.) were used after cleaning by (1) detergent in water and (2) pure water.

Synthesis of elastomer microspheres by surfactant-free emulsion polymerization

All elastomer microspheres were synthesized using a surfactant-free emulsion polymerization technique. For that purpose, a three-neck round-bottom flask (200 mL or 1 L) equipped with a mechanical stirrer, a condenser, and N$_2$ gas inlet was charged with water and the corresponding monomer (BA or EA). The amounts of monomers required in these polymerizations are shown in Table S1.† The subsequent addition of crosslinker DVB resulted in the preparation of crosslinked microspheres. Then, the solution was heated to 70 °C in an oil bath and sparged with N$_2$ (30 min), before the reaction was initiated by addition of the initiator KPS (2 mM; 0.05 g for the preparation of BA(0)500, EA(0)260, EA(0)390, EA(0)710, or 0.27 g for the preparation of BA(0)710, BA(1)410, EA(1)450, BA(5)340) dissolved in water (5 mL). After 24 h, the resulting microsphere dispersions were cooled to room temperature. The thus obtained elastomer microspheres were purified by two cycles of centrifugation/redispersion in water (RCF = ~3000 g; ~5 min), before the microsphere dispersions were dialyzed for 1 week (daily water changes).

Synthesis of polystyrene (PS) microspheres by dispersion polymerization

PS microspheres that adsorb at the air/water interface have previously been reported by Armes.[50] Cationic PS microspheres were prepared by dispersion polymerization of styrene in methanol (initiator: V-50) at 60 °C.[50] A three-neck round-bottom flask (200 mL), equipped with a mechanical stirrer, a condenser, and N$_2$ gas inlet was charged with methanol (85 mL) and styrene (6.9 mL), before the solution was heated to 60 °C and sparged with N$_2$ (30 min). Then, V-50 (0.082 g, 3.3 mM) dissolved in methanol (5 mL) was added to start the reaction. After 24 h, the reaction was stop by cooling the resulting dispersions to room temperature. The thus obtained microsphere dispersions were purified by centrifugation/redispersion (two cycles with methanol and four more cycles with water). For the first two cycles, the dispersions were centrifuged at 3000 rpm for 30 min, and the supernatants were carefully decanted and replaced with methanol. Thereafter, centrifugation/redispersion cycles were conducted at 5000 rpm for 30 min.

Characterization of elastomer microspheres

The hydrodynamic diameters (D_h) of the elastomer and PS microspheres were examined by dynamic light scattering (DLS) measurements (Malvern Instruments Ltd., Zetasizer Nano S, UK). Diameters were calculated using the measured diffusion coefficients and the Stokes–Einstein equation (Zetasizer software v6.12). Dispersion samples (1 mL) containing 0.01 wt% microspheres were used for the measurements of the time-average intensity correlation function with a measurement time of 30 s. The zeta potentials of the microspheres were measured using a Zetasizer Nano ZS instrument (Malvern Instruments Ltd., UK). The Smoluchowski equation was used to analyze the resulting electrophoretic mobilities. The dispersion samples ($\sim$1 mL) were prepared under the same conditions as those used for the DLS measurements (0.01 wt% dispersions). Prior to the DLS and zeta potential measurements, the samples were allowed to thermally equilibrate for 600 s at 25 °C.

Observation of the drying process of microsphere dispersions

The shape of the sessile droplets that contain the microspheres during evaporation of water and the dried structures were evaluated macroscopically using a digital camera (Canon, EOS Kiss ×4). The dispersion droplets (30 μL) were dried at room temperature (25 ± 1 °C) on glass substrates.

The individual microspheres were microscopically examined in aqueous solution using an optical microscope (BX 53, Olympus) equipped with a digital camera (ImageX Earth, ImageX Pro version 3.1.3.0, Kikuchi-Optical Co., Ltd.).

AFM observations of the deformation of elastomer microspheres on solid substrates

A laboratory-built AFM was used in this study; this instrument has previously been described elsewhere.[45,46] The height images in aqueous and dry environment were acquired in tapping mode using a miniaturized cantilever (BL-AC10-DS, Olympus, Japan) with the spring constant of $\sim$0.1 N m^{-1} (resonant frequency: $\sim$600 kHz in water and $\sim$1.2 MHz in air). An amorphous carbon tip, which was grown on the original tip by electron beam deposition, was sharpened (radius: $\sim$4 nm) by plasma etching under an argon atmosphere. The cantilever oscillation was detected by an optical-beam-deflection detector with a red laser (680 nm). For the AFM imaging of the elastomer microspheres, the cantilever free-oscillation amplitude was set to 5–30 nm, and the set-point amplitude was set to 70–90% of the free-oscillation amplitude depending on the state of microsphere. In order to adsorb the negatively charged elastomer microspheres onto a substrate, a mica substrate was modified by 3-aminopropyltriethoxysilane (APTES), which leads to the formation of positively charged surfaces. APTES solution (1 wt%, 3 μL) was dropped on a freshly cleaved mica surface, and after 3 min, the surface was rinsed with pure water to remove any excess APTES. Subsequently, a droplet of the microsphere dispersion (0.1 wt%, 3 μL) was first placed on the positively charged substrate. After 5 min of incubation at room temperature ($\sim$25 °C), the substrate was washed with 100 μL of

pure water. The sample was observed in pure water in the aqueous state or after drying. All AFM imaging was performed at room temperature ($\sim$25 °C) under the following conditions: scanning area = 1500 × 1500 nm^2; 120 × 120 pixels^2; frame rate = 1 fps.

Preparation of the films

Monolayer films of the elastomer microspheres were prepared by transporting the microspheres adsorbed at the air/water interface of a Langmuir trough (trough dimensions: 14 cm × 68 cm; compressible area: 952 cm^2) to a cleaned glass substrate (24 mm × 60 mm; Matsunami Glass Ind., Ltd.) with a tilt angle of 90°. The surface pressure of the air/water interface where the microspheres were adsorbed was measured using a Wilhelmy plate method. To extend the microspheres at the interface of the trough, dispersions of the microspheres in a mixture of water and ethanol (1 : 1) were used. All glass substrates (26 mm × 76 mm/Micro Slide Glass, Matsunami Glass Ind., Ltd.) were used after cleaning by (1) detergent in water and (2) pure water.

Author contributions

Y. S., H. M., and D. S. wrote the draft manuscript. S. H. discovered the ordered arrangement of elastomer microspheres after drying elastomer microsphere dispersions. Y. S. synthesized elastomer microspheres and formed the microsphere films. M. T. contributed to the preparation and investigation of PS microspheres. Y. N. evaluated the elastomer microspheres using AFM. T. U. contributed to the development/tuning of the AFM. The obtained all data were analysed by Y. S. D. S. designed and supervised the study.

Conflicts of interest

The authors declare the absence of any potential conflicts of interest.

Acknowledgements

References

1 N. Vogel, M. Retsch, C.-A. Fustin, A. del Campo and U. Jonas, *Chem. Rev.*, 2015, **115**, 6265–6311.

2 V. Lotito and T. Zambelli, *J. Colloid Interface Sci.*, 2015, **447**, 202–210.

3 S. Fujii and Y. Nakamura, *Langmuir*, 2017, **33**, 7365–7379.

4 R. van Dommelen, P. Fanzio and L. Sasso, *Adv. Colloid Interface Sci.*, 2018, **251**, 97–114.

5 V. Liljeström, C. Chen, P. Dommersnes, J. O. Fossum and A. H. Gröschel, *Curr. Opin. Colloid Interface Sci.*, 2019, **40**, 25–41.

6 H. Jiang, Y. Sheng and T. Ngai, *Curr. Opin. Colloid Interface Sci.*, 2020, **49**, 1–15.

7 M. A. Boles, M. Engel and D. V. Talapin, *Chem. Rev.*, 2016, **116**, 11220–11289.

8 J. Hou, M. Li and Y. Song, *Angew. Chem., Int. Ed.*, 2018, **57**, 2544–2553.

9 A. Kawamura, M. Kohri, G. Morimoto, Y. Nannichi, T. Taniguchi and K. Kishikawa, *Sci. Rep.*, 2016, **6**, 33984.

10 S.-G. Park, S. Y. Lee, S. G. Jang and S.-M. Yang, *Langmuir*, 2010, **26**, 5295–5299.

11 K. R. Phillips, N. Vogel, I. B. Burgess, C. C. Perry and J. Aizenberg, *Langmuir*, 2014, **30**, 7615–7620.

12 J. N. Anker, W. P. Hall, O. Lyandres, N. C. Shah, J. Zhao and R. P. van Duyne, *Nat. Mater.*, 2008, **7**, 442–453.

13 T. Kureha, S. Hiroshige, S. Matsui and D. Suzuki, *Colloids Surf., B*, 2017, **155**, 166–172.

14 L. Bai, Z. Xie, W. Wang, C. Yuan, Y. Zhao, Z. Mu, Q. Zhong and Z. Gu, *ACS Nano*, 2014, **8**, 11094–11100.

15 Y. Huang, W. Li, M. Qin, H. Zhou, X. Zhang, F. Li and Y. Song, *Small*, 2017, **13**, 1503339.

16 R. Contreras-Cáceres, A. Sánchez-Iglesias, M. Karg, I. Pastoriza-Santos, J. Pérez-Juste, J. Pacifico, T. Hellweg, A. Fernández-Barbero and L. M. Liz-Marzán, *Adv. Mater.*, 2008, **20**, 1666–1670.

17 M. Yue, Y. Hoshino and Y. Miura, *Chem. Sci.*, 2015, **6**, 6112–6123.

18 S. Hiroshige, T. Kureha, D. Aoki, J. Sawada, D. Aoki, T. Takata and D. Suzuki, *Chem.–Eur. J.*, 2017, **23**, 8405–8408.

19 S. Hiroshige, J. Sawada, D. Aoki, T. Takata and D. Suzuki, *J. Soc. Rheol., Jpn.*, 2019, **47**, 051–054.

20 T. Kureha, S. Hiroshige, D. Suzuki, J. Sawada, D. Aoki, T. Takata and M. Shibayama, *Langmuir*, 2020, **36**, 4855–4862.

21 S. Hiroshige, H. Minato, Y. Nishizawa, Y. Sasaki, T. Kureha, M. Shibayama, K. Uenishi, T. Takata and D. Suzuki, *Polym. J.*, 2021, **53**, 345–353.

22 M. Rey, T. Yu, R. Guenther, K. Bley and N. Vogel, *Langmuir*, 2019, **35**, 95–103.

23 X. Yan, J. Yao, G. Lu, X. Li, J. Zhang, K. Han and B. Yang, *J. Am. Chem. Soc.*, 2005, **127**, 7688–7689.

24 P. Jiang and M. J. McFarland, *J. Am. Chem. Soc.*, 2005, **127**, 3710–3711.

25 L. Isa, K. Kumar, M. Müller, J. Grolig, M. Textor and E. Reimhult, *ACS Nano*, 2010, **4**, 5665–5670.

26 Y. Li, P. Chen, Y. Wang, S. Yan, X. Feng, W. Du, S. A. Koehler, U. Demirci and B. F. Liu, *Adv. Mater.*, 2016, **28**, 3543–3548.

27 K. Uhlig, T. Wegener, J. He, M. Zeiser, J. Bookhold, I. Dewald, N. Godino, M. Jaeger, T. Hellweg, A. Fery and C. Duschl, *Biomacromolecules*, 2016, **17**, 1110–1116.

28 K. Horigome and D. Suzuki, *Langmuir*, 2012, **28**, 12962–12970.

29 M. Anyfantakis and D. Baigl, *Angew. Chem., Int. Ed.*, 2014, **53**, 14077–14081.

30 D. Mampallil and H. B. Eral, *Adv. Colloid Interface Sci.*, 2018, **252**, 38–54.

31 H. Minato, M. Murai, T. Watanabe, S. Matsui, M. Takizawa, T. Kureha and D. Suzuki, *Chem. Commun.*, 2018, **54**, 932–935.

32 M. Takizawa, Y. Sazuka, K. Horigome, Y. Sakurai, S. Matsui, H. Minato, T. Kureha and D. Suzuki, *Langmuir*, 2018, **34**, 4515–4525.

33 H. Minato, M. Takizawa, S. Hiroshige and D. Suzuki, *Langmuir*, 2019, **35**, 10412–10423.

34 M. Karg, A. Pich, T. Hellweg, T. Hoare, L. A. Lyon, J. J. Crassous, D. Suzuki, R. A. Gumerov, S. Schneider, I. I. Potemkin and W. Richtering, *Langmuir*, 2019, **35**, 6231–6255.

35 R. D. Deegan, O. Bakajin, T. F. Dupont, G. Huber, S. R. Nagel and T. A. Witten, *Nature*, 1997, **389**, 827–829.

36 D. Suzuki and H. Kawaguchi, *Colloid Polym. Sci.*, 2006, **284**, 1471–1476.

37 H. Hu and R. G. Larson, *Langmuir*, 2005, **21**, 3972–3980.

38 P. Hanarp, D. S. Sutherland, J. Gold and B. Kasemo, *Colloids Surf., A*, 2003, **214**, 23–36.

39 S. Venkatesh and P. Jiang, *Langmuir*, 2007, **23**, 8231–8235.

40 A. Plettl, F. Enderle, M. Saitner, A. Manzke, C. Pfahler, S. Wiedemann and P. Ziemann, *Adv. Funct. Mater.*, 2009, **19**, 3279–3284.

41 N. Vogel, C. Fernández-López, J. Pérez-Juste, L. M. Liz-Marzán, K. Landfester and C. K. Weiss, *Langmuir*, 2012, **28**, 8985–8993.

42 P. Pieranski, *Phys. Rev. Lett.*, 1980, **45**, 569–572.

43 T. Ando, N. Kodera, E. Takai, D. Maruyama, K. Saito and A. Toda, *Proc. Natl. Acad. Sci. U. S. A.*, 2001, **98**, 12468–12472.

44 T. Ando, T. Uchihashi and T. Fukuma, *Prog. Surf. Sci.*, 2008, **83**, 337–437.

45 T. Ando, T. Uchihashi and S. Scheuring, *Chem. Rev.*, 2014, **114**, 3120–3188.

46 Y. Nishizawa, S. Matsui, K. Urayama, T. Kureha, M. Shibayama, T. Uchihashi and D. Suzuki, *Angew. Chem., Int. Ed.*, 2019, **58**, 8809–8813.

47 H. Minato, Y. Nishizawa, T. Uchihashi and D. Suzuki, *Polym. J.*, 2020, **52**, 1137–1141.

48 S. Matsui, T. Kureha, S. Hiroshige, M. Shibata, T. Uchihashi and D. Suzuki, *Angew. Chem., Int. Ed.*, 2017, **56**, 12146–12149.

49 J. N. Israelachvili, *Intermolecular and surface forces*, Academic Press, Cambridge, MA, 3rd edn, 2011.

50 S. L. Kettlewell, A. Schmid, S. Fujii, D. Dupin and S. P. Armes, *Langmuir*, 2007, **23**, 11381–11386.